

## Géographie physique et Quaternaire



# Floodplain Chronology and Vertical Sedimentation Rates Along the Red River, Southern Manitoba

## Chronologie de la plaine d'inondation de la rivière Rouge (sud du Manitoba) et taux de sédimentation verticale

## Cronología de las inundaciones de las praderas y tasa vertical de sedimentación a lo largo de Red River al sur de Manitoba

Gregory R. Brooks

Volume 56, numéro 2-3, 2002

Drylands: Holocene Climatic, Geomorphic and Cultural Change on the Canadian Prairies

URI : <https://id.erudit.org/iderudit/009103ar>

DOI : <https://doi.org/10.7202/009103ar>

[Aller au sommaire du numéro](#)

### Éditeur(s)

Les Presses de l'Université de Montréal

### ISSN

0705-7199 (imprimé)  
1492-143X (numérique)

[Découvrir la revue](#)

### Citer cet article

Brooks, G. R. (2002). Floodplain Chronology and Vertical Sedimentation Rates Along the Red River, Southern Manitoba. *Géographie physique et Quaternaire*, 56(2-3), 171-180. <https://doi.org/10.7202/009103ar>

### Résumé de l'article

On traite ici des dates au radiocarbone SMA provenant d'échantillons consistant en un os et 38 charbons recueillis dans 12 coupes effectuées le long de la rivière Rouge et de leur contexte géomorphologique. Les dates stratigraphiquement les plus anciennes s'étalement entre 3760 à 6710 étal. BP et démontrent que des dépôts d'inondation datant au moins de l'Holocène moyen sont conservés le long du fond de la vallée. Le taux moyen de migration latérale du chenal au méandre situé près de la coupe Ju30-1-98 est de 0,08 m a<sup>-1</sup> depuis les 3850 dernières années. Dans les coupes Se04-1-97, Ju30-1-98, Ju23-1-98 et Ju21-2-98, le taux de sédimentation verticale au-dessus et en dessous de 1 à 3 m de profondeur varie entre 0,3 et 0,08 mm a<sup>-1</sup> et entre 1,7 et 3,7 mm a<sup>-1</sup>, respectivement. La diminution du taux de sédimentation indique le passage d'un alluvionnement oblique du lit majeur proximal au chenal à une accumulation dans le lit majeur distal au chenal. Dans les coupes Ju28-1-98, Au05-1-00, Au03-1-98 et Ju21-1-98, qui datent de l'Holocène supérieur, le taux de sédimentation verticale varie entre 1,8 et 3,9 mm a<sup>-1</sup>. Un seuil jouet en plastique et deux dates au radiocarbone provenant de la coupe Au05-1-00 témoignent d'une augmentation de 1,6 à 14,3 mm a<sup>-1</sup> du taux de sédimentation récent, probablement en raison d'une érosion fluviatile accentuée par l'agriculture pratiquée à grande échelle depuis le XIX<sup>e</sup> siècle.

# FLOODPLAIN CHRONOLOGY AND VERTICAL SEDIMENTATION RATES ALONG THE RED RIVER, SOUTHERN MANITOBA\*

Gregory R. BROOKS\*\*, Geological Survey of Canada, Natural Resources Canada, 601 Booth Street, Ottawa, Ontario K1A 0E8.

**ABSTRACT** This paper reports the accelerator mass spectrometry radiocarbon ages and geomorphic context of one bone and 38 charcoal samples collected from 12 floodplain exposures along the Red River, southern Manitoba. The stratigraphically oldest dates range from 3760 to 6710 cal BP and indicate that floodplain deposits of at least mid-Holocene age are preserved along the valley bottom. The average rate of lateral channel migration at the meander adjacent to section Ju30-1-98 is up to 0.08 m a<sup>-1</sup> over the past 3850 years. In sections Se04-1-97, Ju30-1-98, Ju23-1-98 and Ju21-2-98, the rates of vertical sedimentation above and below 1 to 3 m depth, range from 0.3 to 0.8 mm a<sup>-1</sup> and 1.7 to 3.7 mm a<sup>-1</sup>, respectively. The decrease in sedimentation rates is interpreted to represent a shift from oblique accretion/proximal overbank sedimentation to distal overbank sedimentation. In sections Ju28-1-98, Au05-1-00, Au03-1-98 and Ju21-1-98, which are late Holocene in age, the average rates of vertical sedimentation range from 1.8 to 3.9 mm a<sup>-1</sup>. A toy plastic pail and two radiocarbon ages from section Au05-1-00 reveal an increase in modern sedimentation rates from 1.6 to 14.3 mm a<sup>-1</sup>. This increase may have been caused by greater fluvial erosion from the large-scale introduction of European agricultural practices in the 19<sup>th</sup> century.

**RÉSUMÉ** Chronologie de la plaine d'inondation de la rivière Rouge (sud du Manitoba) et taux de sédimentation verticale. On traite ici des dates au radiocarbone SMA provenant d'échantillons consistant en un os et 38 charbons recueillis dans 12 coupes effectuées le long de la rivière Rouge et de leur contexte géomorphologique. Les dates stratigraphiquement les plus anciennes s'étaient entre 3760 à 6710 étal. BP et démontrent que des dépôts d'inondation datant au moins de l'Holocène moyen sont conservés le long du fond de la vallée. Le taux moyen de migration latérale du chenal au méandre situé près de la coupe Ju30-1-98 est de 0,08 m a<sup>-1</sup> depuis les 3850 dernières années. Dans les coupes Se04-1-97, Ju30-1-98, Ju23-1-98 et Ju21-2-98, le taux de sédimentation verticale au-dessus et en dessous de 1 à 3 m de profondeur varie entre 0,3 et 0,08 mm a<sup>-1</sup> et entre 1,7 et 3,7 mm a<sup>-1</sup>, respectivement. La diminution du taux de sédimentation indique le passage d'un alluvionnement oblique du lit majeur proximal au chenal à une accumulation dans le lit majeur distal au chenal. Dans les coupes Ju28-1-98, Au05-1-00, Au03-1-98 et Ju21-1-98, qui datent de l'Holocène supérieur, le taux de sédimentation verticale varie entre 1,8 et 3,9 mm a<sup>-1</sup>. Un seau jouet en plastique et deux dates au radiocarbone provenant de la coupe Au05-1-00 témoignent d'une augmentation de 1,6 à 14,3 mm a<sup>-1</sup> du taux de sédimentation récent, probablement en raison d'une érosion fluviatile accentuée par l'agriculture pratiquée à grande échelle depuis le XIX<sup>e</sup> siècle.

**RESUMEN** Cronología de las inundaciones de las praderas y tasa vertical de sedimentación a lo largo de Red River al sur de Manitoba. Este manuscrito presenta la datación con radiocarbono obtenida a través de la espectrometría de acelerador de masa y del estudio geomorfológico de un hueso y de 38 muestras de carbón colectadas en 12 sitios que sufrieron inundaciones en las planicies a lo largo de Red River al sur de Manitoba. Las edades estratigráficas más antiguas se sitúan dentro del rango de 3760 a 6710 años anteriores al presente e indican que los depósitos de inundaciones de las planicies que corresponden al Holoceno medio se han conservado en el fondo del valle. La tasa media de desplazamiento lateral del canal en el meandro adyacente de la sección Ju30-1-98 abarca cerca de 0,08 m a<sup>-1</sup> en los últimos 3850 años. En las secciones Se04-1-97, Ju30-1-98, Ju23-1-98 y Ju21-2-98, la tasa de sedimentación vertical por encima y por debajo de 1 a 3 m de profundidad, varía dentro del rango de 0,3 a 0,8 mm a<sup>-1</sup> y 1,7 a 3,7 mm a<sup>-1</sup>, respectivamente. Se considera que la disminución de la tasa de sedimentación se relaciona con el paso de la sedimentación de acreción oblicua proximal del lecho fluvial a una sedimentación de tipo distal del lecho principal del canal. En las secciones Ju28-1-98, Au05-1-00, Au05-1-00, Au03-1-98 y Ju21-1-98, que datan del Holoceno superior, la tasa promedio de la sedimentación vertical varía entre 1,8 a 3,9 mm a<sup>-1</sup>. Un cubo de plástico de juguete y dos dataciones con radiocarbono de la sección Au05-1-00 revelan un aumento en la tasa actual de sedimentación de 1,6 a 14,3 mm a<sup>-1</sup>. Este incremento puede haber sido causado por una erosión fluvial más pronunciada provocada por la introducción a larga escala de prácticas agrícolas europeas durante el siglo XIX.

Manuscrit reçu le 26 janvier 2003 ; manuscrit révisé accepté le 23 juillet 2003 (publié en mai 2004)

\*Geological Survey of Canada Contribution 2002228

\*\*E-mail address: gbrooks@nrcan.gc.ca

## INTRODUCTION

The chronology, outlet history and deposits of Glacial Lake Agassiz in Manitoba have received considerable attention in the literature (e.g., Upham, 1895; Johnson, 1946; Teller, 1976; Teller and Clayton, 1983; Teller, 2001), but there are comparatively few published studies of the Red River alluvium or geomorphology. Of these, Nielsen *et al.* (1993) present stratigraphical, chronological and paleoecological data from river bank sections between Winnipeg and St. Andrews. Rannie *et al.* (1989) summarize the Holocene evolution of the lower Assiniboine River, a major tributary of the Red River (Fig. 1a), while Rannie (1990) describes the deposits and morphology of the low-angled alluvial fan associated with the lower Assiniboine River. More recently, Brooks (2003a and b) summarizes the Red River floodplain sedimentology and floodplain evolution at two meanders near St. Jean Baptiste, Manitoba.

This paper reports the accelerator mass spectrometry radiocarbon ages and geomorphic context of one bone and 38 charcoal samples collected from 12 exposures of the Red River floodplain between Emerson and St. Adolphe, Manitoba (Fig. 1). The samples were collected to elucidate the general chronology and stratigraphy of the Red River floodplain in southern Manitoba. In addition to increasing the understanding of Holocene fluvial activities of a major river on the eastern Canadian prairies, the paper provides insights into the floodplain chronology and vertical sedimentation rates of a mud-dominated stream, a river type that has received little attention in the geomorphic literature compared to sand- and gravel-bed rivers (Brooks, 2003a).

## RED RIVER FLOODPLAIN AND DEPOSITS

The geomorphic setting of the Red River (known as the Red River of the North in the United States) is described by Brooks and Nielsen (2000) and Brooks (2003a and b) and need not be repeated here. Of specific relevance, the river occupies a shallow alluvial valley, up to 15 m deep (to the thalweg) and 2 500 m wide (Brooks and Nielsen, 2000). The predominately silt deposits within this valley represent the genetic floodplain of the river and are the product of alluvial sedimentation (see Brooks, 2003a and b). The floodplain alluvium ranges from 15 to 22 m deep in ten boreholes at two meanders located near St. Jean Baptiste, Manitoba (Brooks, 2003b). Although gently undulatory, the floodplain surface gradually increases in height from the proximal to distal areas with respect to the actively accreting portion of a given meander. Development of the river began in southern Manitoba between 7800 and 8200 BP (~8900 cal BP; Teller *et al.*, 1996) following the final recession of Glacial Lake Agassiz (see Teller and Clayton, 1983; Teller *et al.*, 1996).

A function of a low rate of lateral channel migration (Brooks, 2003b), there are few bank exposures of the Red River floodplain compared to along more active sand and sand-gravel bed rivers. The 12 sites reported in this paper are a subset of 32 floodplain and valley side exposures that were logged in 1997, 1998 and 2000 between Emerson and St. Adolphe (Fig. 1). The bank deposits at all 12 logged exposures are similar sedimentologically. Silt-rich overbank deposits forming the

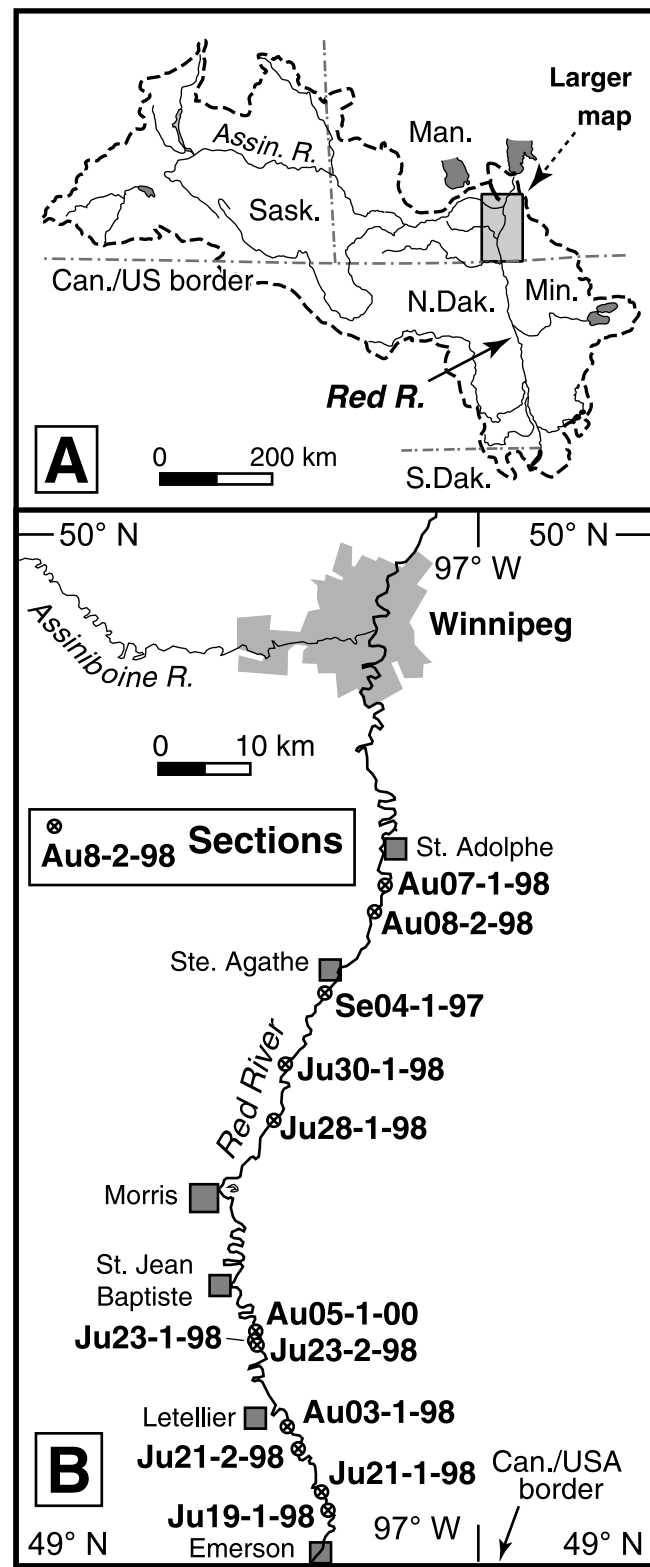


FIGURE 1. Maps showing (A) the Red River drainage basin and (B) the 12 floodplain sections along the Red River, southern Manitoba.  
Le bassin versant de la rivière Rouge (A) et les douze coupes situées le long de la plaine d'inondation de la rivière Rouge (B), dans le sud du Manitoba.

upper 2 to 3 m of the bank are generally weakly defined and composed of massive beds and laminations (Fig. 2; Brooks, 2003a). Underlying these are oblique accretion deposits (see Nanson and Croke, 1992; Page *et al.*, 2003) that are similar texturally and structurally; the transition between the two is gradational and indistinct (Brooks, 2003a). In a given section, differentiating between overbank and oblique accretion deposits in a given section generally must be inferred based on the approximate height range and character of modern sedimentation proximal to the river. No major unconformities were identified in any of the exposures.

Alluvial deposits also form "benches" and "terraces" that are commonly exposed along the concave banks of the meanders and on both sides of straight, stable reaches of channel. These deposits, however, represent modern alluvium aggraded on the toes of low-angled, very slow moving (up to  $\sim 1 \text{ m a}^{-1}$  displacement) landslides formed in alluvium or glaciolacustrine deposits. As such, these are not floodplain deposits in

the sense of long-term alluvial storage in the valley bottom. The bench and terrace surfaces are discontinuous and irregular topographically, commonly stepping up and down in height both towards and along the channel, and can easily be confused with the "true" floodplain deposits. None of the dated samples were collected from the benches and terraces.

## RADIOCARBON AGES

The 39 radiocarbon ages are listed in Table I. All but one of these were obtained from charcoal samples; the non-charcoal sample is derived from *Bison* teeth. The large proportion of dates from charcoal samples reflects its relatively common occurrence in the floodplain deposits as isolated fragments, fragments in linear alignments, or concentrations in lenses, laminations or within heat-altered, reddish-stained sediments (the latter are hearths; see Lian and Brooks, 2004). All of the dated samples represent maximum ages for the encapsulating

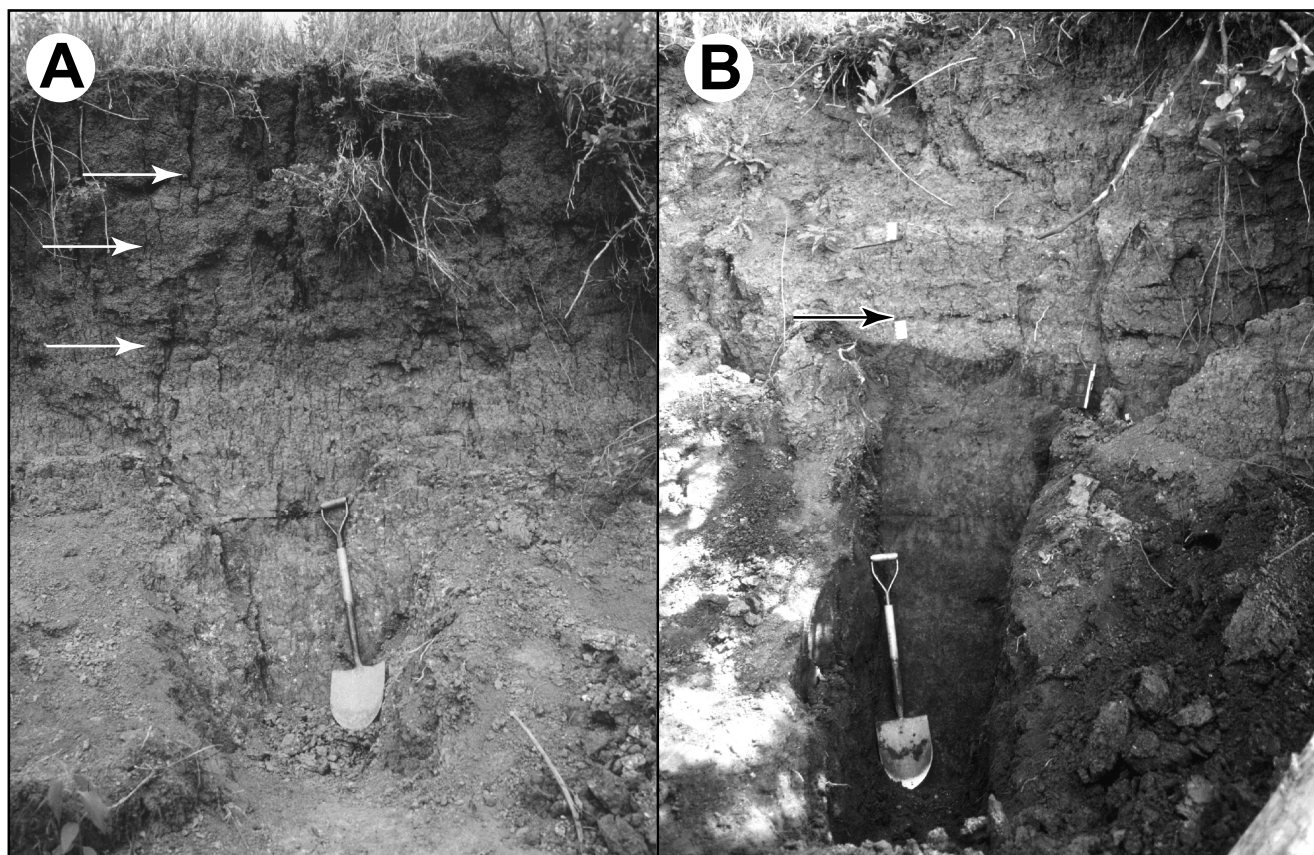


FIGURE 2. Photographs of sections Ju30-1-98 (A) and Ju28-1-98 (B). Section Ju30-1-98 represents one of the mid-Holocene aged sections and contains buried paleosols (marked by arrows). The darker shading in the upper portion of the exposure (above lowest arrow) reflects pedological development in an aggrading floodplain setting. Section Ju28-1-98 consists of late Holocene deposits and lacks buried paleosols and pedological development. Note, the buried charcoal layer marked by an arrow.

*Photographies des coupes Ju30-1-98 (A) et Ju28-1-98 (B). La coupe Ju30-1-98 montre des éléments datant de l'Holocène moyen et comprend des paléosols enfouis (indiqués par les flèches). La partie ombragée plus foncée (au-dessus de la flèche la plus basse) témoigne d'un développement de profil dans un milieu de plaine d'inondation en voie d'alluvionnement. La coupe Ju28-1-98 est composée de dépôts de l'Holocène supérieur et ne comprend ni paléosol enfoui ni développement de profil. Noter la couche de charbon enfouie indiquée par la flèche.*

TABLE I  
*Radiocarbon dates*

| Sample location | Latitude/<br>Longitude         | Depth<br>(m)     | Material                    | Laboratory<br>number | $^{13}\text{C}/^{12}\text{C}$ ratio<br>(0/00) | Radiocarbon age<br>(years BP) | Calibrated age and age<br>range at $1\sigma$<br>(years before AD 2000) |
|-----------------|--------------------------------|------------------|-----------------------------|----------------------|---|-------------------------------|--|
| Au07-1-98       | 49° 38' 42" N<br>97° 07' 00" W | 1.6              | charcoal <sup>a</sup>       | TO-7572              | -25.0   | 4180 ± 60                     | 4770 (4630-4880) <sup>b</sup>  |
| "               | "                              | 3-4 <sup>c</sup> | "                           | TO-7574              | -25.0   | 5840 ± 70                     | 6710 (6610-6780)   |
| "               | "                              | 3-4 <sup>c</sup> | "                           | TO-7575              | -25.0   | 5670 ± 60                     | 6480 (6410-6560) <sup>b</sup>  |
| Au08-2-98       | 49° 37' 16" N<br>97° 07' 47" W | 1.7              | charcoal <sup>a</sup>       | TO-7833              | -25.0   | 3000 ± 60                     | 3240 (3130-3370) <sup>b</sup>  |
| Se04-1-97       | 49° 32' 39" N<br>97° 12' 08" W | 1.05             | charcoal <sup>a</sup>       | TO-6980              | -25.0   | 2910 ± 90                     | 3080 (2940-3260) <sup>b</sup>  |
| "               | "                              | 2.4              | "                           | TO-6976              | -25.0   | 4040 ± 110                    | 4530 (4460-4860) <sup>b</sup>  |
| "               | "                              | 4.2              | "                           | TO-6979              | -25.0   | 4400 ± 80                     | 5020 (4910-5260) <sup>b</sup>  |
| "               | "                              | 5.7              | teeth of Bison <sup>d</sup> | TO-6733              | -25.0   | 5430 ± 70                     | 6290 (6170-6340) <sup>b</sup>  |
| "               | "                              | 6.3              | "                           | TO-6977              | -25.0   | 5430 ± 70                     | 6290 (6170-6340) <sup>b</sup>  |
| "               | "                              | 6.3              | "                           | TO-6978              | -25.0   | modern                        | na   |
| "               | "                              | 8.4              | "                           | TO-6981              | -25.0   | 3870 ± 110                    | 4350 (4150-4470) <sup>b</sup>  |
| Ju30-1-98       | 49° 28' 26" N<br>97° 15' 33" W | 1.9              | charcoal <sup>a</sup>       | TO-7832              | -25.0   | 3120 ± 110                    | 3410 (3260-3520)   |
| "               | "                              | 4.22             | "                           | TO-7831              | -25.0   | 3810 ± 110                    | 4250 (4040-4460) <sup>b</sup>  |
| "               | "                              | 4.22             | "                           | TO-7830              | -25.0   | 3540 ± 110                    | 3850 (3700-4030) <sup>b</sup>  |
| Ju28-1-98       | 49° 25' 24" N<br>97° 16' 37" W | 0.83             | charcoal <sup>a</sup>       | TO-7509              | -25.0   | 570 ± 50                      | 640 (580-690) <sup>b</sup>   |
| Ju28-1-98       |                                | 0.98             | "                           | TO-7510              | -25.0   | 630 ± 50                      | 650 (600-710) <sup>b</sup>   |
| "               |                                | 1.36             | "                           | TO-7511              | -25.0   | 800 ± 60                      | 740 (720-810)  |
| "               |                                | 1.65             | "                           | GSC-6347             | -24.1   | 900 ± 50 <sup>e</sup>         | 840 (810-960)  |
| "               |                                | 1.65             | "                           | TO-7512              | -25.0   | 1060 ± 60                     | 1010 (980-1100)  |
| "               |                                | 2.2              | "                           | TO-7513              | -25.0   | 1170 ± 120                    | 1110 (1000-1310)   |
| "               |                                | 2.68             | "                           | TO-7514              | -25.0   | 1610 ± 50                     | 1570 (1470-1590)   |
| Au05-1-00       | 49° 13.4' N<br>97° 17' 1" W    | 1.2              | charcoal <sup>a</sup>       | Beta-161762          | -27.4   | 200 ± 40                      | 250 (200-340) <sup>b</sup>   |
| "               | "                              | 1.45             | "                           | Beta-161761          | -29.4   | 330 ± 40                      | 430 (360-520) <sup>b</sup>   |
| Ju23-1-98       | 49° 12' 48" N<br>97° 18' 15" W | 1.5              | charcoal <sup>a</sup>       | TO-7768              | -25.0   | 2470 ± 60                     | 2670 (2410-2770) <sup>b</sup>  |
| "               | "                              | 3.8              | "                           | TO-7769              | -25.0   | 4010 ± 110                    | 4530 (4350-4840) <sup>b</sup>  |
| "               | "                              | 4.3              | "                           | TO-7770              | -25.0   | 3740 ± 50                     | 4140 (4040-4200)   |
| "               | "                              | 5.2              | "                           | TO-7771              | -25.0   | 4340 ± 70                     | 4920 (4890-5080)   |
| Ju23-2-98       | 49° 12' 35" N<br>97° 17' 59" W | 2.3              | charcoal <sup>a</sup>       | TO-7577              | -25.0   | 2380 ± 80                     | 2410 (2390-2760)   |
| "               | "                              | 4.25             | "                           | TO-7576              | -25.0   | 3470 ± 110                    | 3760 (3640-3920) <sup>b</sup>  |
| Au03-1-98       | 49° 8' 16" N<br>97° 15' 19" W  | 1.22             | charcoal <sup>a</sup>       | TO-7578              | -25.0   | 1600 ± 70                     | 1570 (1460-1600)   |
| "               | "                              | 3.05             | charcoal <sup>f</sup>       | TO-9653              | -25.0   | 1170 ± 40                     | 1110 (1010-1250)   |
| "               | "                              | 3.55             | charcoal <sup>a</sup>       | TO-7579              | -25.0   | 1780 ± 110                    | 1760 (1600-1910)   |
| Ju21-2-98       | 49° 06' 41" N<br>97° 14' 30" W | 1.45             | charcoal <sup>a</sup>       | TO-7829              | -25.0   | 1490 ± 100                    | 1400 (1340-1570)   |

TABLE I (suite)  
Radiocarbon dates

| Sample location | Latitude/<br>Longitude         | Depth<br>(m) | Material              | Laboratory<br>number | $^{13}\text{C}/^{12}\text{C}$ ratio<br>(0/00) | Radiocarbon age<br>(years BP) | Calibrated age and age<br>range at $1\sigma$<br>(years before AD 2000) |
|-----------------|--------------------------------|--------------|-----------------------|----------------------|---|-------------------------------|--|
| "               | "                              | 2.7          | "                     | TO-7828              | -25.0   | $3360 \pm 120$                | 3660 (3520-3860) <sup>b</sup>  |
| "               | "                              | 5.5          | "                     | TO-7827              | -25.0   | $4010 \pm 100$                | 4530 (4410-4830) <sup>b</sup>  |
| Ju21-1-98       | 49° 04' 12" N<br>97° 12' 18" W | 1.9          | charcoal <sup>a</sup> | TO-7772              | -25.0   | $900 \pm 50$                  | 840 (790-960)  |
| Ju19-1-98       | 49° 03' 06" N<br>97° 11' 47" W | 2.45         | charcoal <sup>a</sup> | TO-7773              | -25.0   | $1180 \pm 50$                 | 1120 (1060-1220)   |
| "               | "                              | 2.15         | charcoal <sup>a</sup> | TO-7826              | -25.0   | $2230 \pm 60$                 | 2280 (2200-2390) <sup>b</sup>  |
| "               | "                              | 5.7          | "                     | TO-7825              | -25.0   | $4100 \pm 60$                 | 4630 (4500-4860) <sup>b</sup>  |

a Collected by G.R. Brooks

b Age represents the mean of up to multiple intercepts with the calibration curve

c Samples TO-7574 and TO-7575 were obtained about 30-35 m downstream of the measured section. This depth range represents the approximate equivalent depth at the measured section, as mentioned in the text

d Identified by R.E. Morlan (personal communication, 1998)

e The error range of this age is expressed at  $2\sigma$

f Collected by O.B. Lian

deposits at the respective sampling depths. Samples were selected carefully to favour "fresh looking" charcoal to avoid dating material that experienced long distance transport and multiple reworking. Nevertheless, none of the dated charcoal samples are derived from organic material in growth position and thus all are possibly reworked. Reworked material, however, can be recognized within a given section when a charcoal sample from a stratigraphically younger depth yields a radiocarbon age that is significantly older (beyond the  $2\sigma$  error range) than an underlying dated sample or when one of two samples from the same sampling depth yields a significantly older radiocarbon age than the other. Calibrations of the radiocarbon ages to sidereal years (years before AD 2000) are also listed in Table I, and were determined using calib 4.3 (Stuiver and Reimer, 1993) and the calibration dataset of Stuiver *et al.* (1998).

Inspection of Table I reveals that the majority of the ages within a given section increase with depth as is consistent with the stratigraphy of an aggrading floodplain surface. In most cases where there is transposition the ages generally are similar when the  $2\sigma$  error ranges are compared. However, there are some examples of reworked ages and in addition some other samples warrant a brief qualifying comment, as follows.

The sample depths from section Se04-1-97 are measured with respect to the contact between the deposits of an artificial earthen dyke present at the bank edge and the underlying overbank deposits. Within the sequence of seven dated samples from this section (Fig. 1), the ages of two of the three deepest charcoal samples (modern and  $3870 \pm 110$  BP; Table I) are

transposed relative to the depth positions of the other ages. These two dates evidently were contained within slumped bank materials that were not recognized as such at the time of sampling. The dates thus are interpreted to be unrepresentative of the *in situ* bank deposit ages at the respective sampling depths and will not be referred to in subsequent discussion.

In addition to the two radiocarbon ages collected from section Au03-1-98 ( $1600 \pm 70$  and  $1780 \pm 110$  BP), a third radiocarbon age,  $1170 \pm 40$  BP (Table I), was obtained from charcoal contained within a hearth located about 5 m upstream of the measured section at an equivalent depth of 3.05 m (see Lian and Brooks, 2004). The depth of this age (3.05 m) is transposed stratigraphically with that of the  $1600 \pm 70$  BP aged charcoal sample obtained at 1.22 m. The  $1600 \pm 70$  BP age is interpreted to be based on reworked charcoal and thus is unrepresentative of the encapsulating deposits at the sampling depth.

In section Au07-1-98 (Fig. 1; Table I), charcoal samples aged  $5840 \pm 70$  and  $5670 \pm 60$  BP were collected along a cut-bank face 30-35 m downstream of the measured section. These were encapsulated within large-scale cross-beds interpreted to represent oblique accretion deposits (see Brooks, 2003a). The lateral extensions of these cross-beds are situated within the measured section at an equivalent depth range of 3 to 4 m, but slumping along the bank face between the section and the sampling location precluded a more precise determination of depth. Although the sequencing of the two ages is transposed vertically, the two ages are statistically indistinguishable at a  $2\sigma$  error range.

## RESULTS AND DISCUSSION

### LATERAL CHANNEL MIGRATION

Along many Red River meanders, a ridge and swale pattern is visible on some sets of aerial photographs taken during the spring, when variations in ground moisture conditions and/or stage of vegetation growth help accentuate the pattern (Fig. 3). Where present, a ridge and swale pattern delineates past positions of the convex bank of a meander across the floodplain. As noted by Brooks and Nielsen (2000) and Brooks (2003a), the majority of Red River meanders exhibit only a single ridge and swale sequence of meander growth as opposed to multiple patterns associated with separate episodes of migration.

Sections Au07-1-98, Se04-1-97, Ju30-1-98, Ju23-1-98, Ju-23-2-98, Ju21-2-98 and Ju19-1-98 are located at the upstream sides of meanders where downvalley rotation of the immediately preceding meander is causing the channel to truncate and expose older floodplain deposits (Fig. 3). The stratigraphically oldest dates from these sections are mid-Holocene in age, ranging from 3760 to 6710 cal BP (Table I). Subsequent aggradation above these dated samples has gradually thickened

the floodplain as the meander continued to migrate laterally across the valley bottom. The depth (less than 6.2 m) of the stratigraphically oldest ages, however, is comparatively shallow relative to the overall depth of the floodplain alluvium (e.g., the floodplain alluvium ranges from 15-22 m deep near St. Jean Baptiste; see Brooks, 2003b). The earliest stages of convex bank sedimentation, which aggraded the underlying alluvium, thus may significantly pre-date these ages. The stratigraphically oldest dates thus are interpreted to represent minimum ages for the initiation of convex bank aggradation at the specific location of each section. As an example, Brooks (2003b) only considered dated wood samples collected from core below a depth of 9 m to be representative of the initial age of convex bank formation at two meanders near St. Jean Baptiste (Fig. 1). In one of these cores, a sample collected at 4.2 m depth is 550 years younger than the average age (1010 cal BP) of five closely-constrained dates situated between a depth range 9 to 20 m. Nevertheless, the stratigraphically oldest ages from sections Au07-1-98, Se04-1-97, Ju30-1-98, Ju23-1-98, Ju-23-2-98, Ju21-2-98 and Ju19-1-98 reveal that floodplain deposits of at least mid-Holocene age are preserved along the valley bottom, as is implied by the single episode of lateral growth, based on the ridge and swale patterns at most of the meanders along the river.

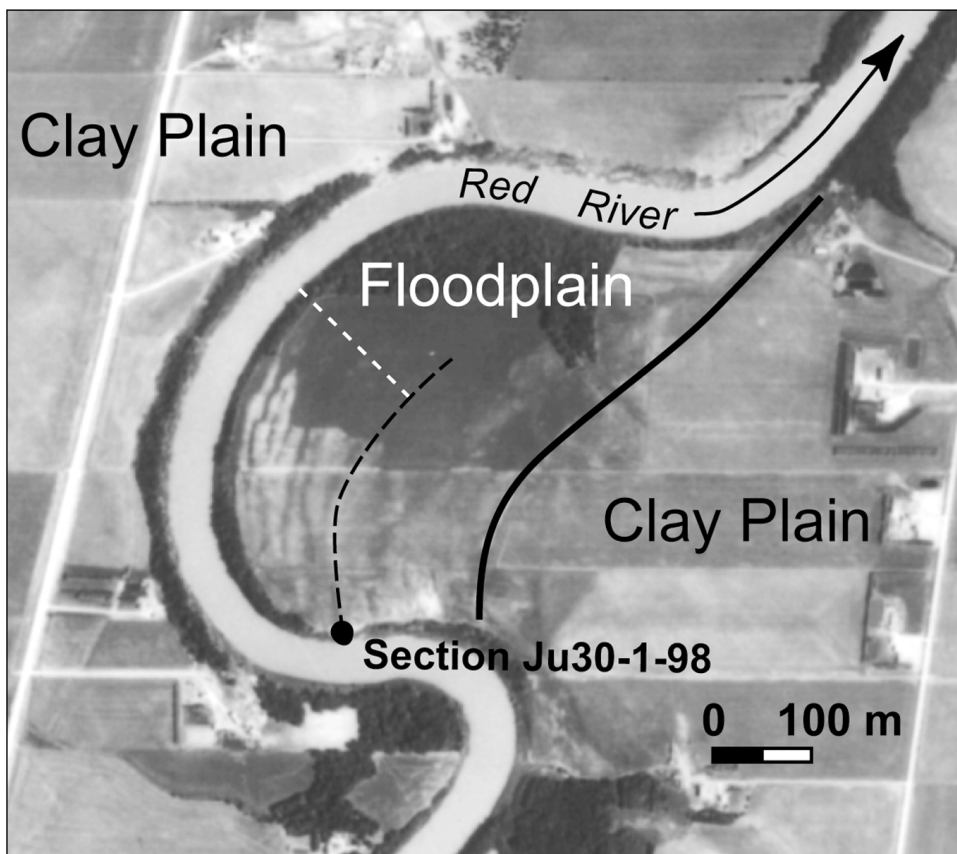


FIGURE 3. Aerial photograph of the meander adjacent to section Ju30-1-98 (NAPL A25475-170). Note, the arcuate shading on the floodplain approximately paralleling the channel that marks the ridge and swale pattern. This pattern is truncated by lateral channel erosion at the upstream portion of the meander. An isoline marks (black dashed line) the approximate position of the convex bank that corresponds approximately to the location of section Ju30-1-98. The white dashed line indicates where distance was measured to estimate the rate of lateral channel migration (which was measured on a rectified photomosaic map rather than on this image).

Photographie aérienne du méandre situé près de la coupe Ju30-1-98 (NAPL A25475-170). Noter la partie ombragée en arcs à peu près parallèles au chenal qui indiquent la topographie en creux et en bosses, topographie interrompue par l'érosion latérale du chenal dans la partie aval du méandre. Une isoligne (tirets noirs) identifie la position approximative de la rive convexe qui correspond à peu près à l'emplacement de la coupe Ju30-1-98. Les tirets blancs identifient l'endroit d'où les mesures ont été prises afin d'estimer le taux de migration latérale du chenal (à partir de la photomosaïque corrigée et non pas de cette photographie).

Although a ridge and swale pattern commonly is present on the floodplain, only at the meander adjacent to section Ju30-1-98 can the pattern be readily used to estimate a long-term rate of lateral channel migration. At the other sites, the ridge and swale pattern is poorly defined, obscured by foliage and/or poorly aligned relative to the location of the logged section. At section Ju30-1-98, two charcoal samples were collected at a depth of 4.22 m and yielded radiocarbon ages of  $3810 \pm 110$  and  $3540 \pm 110$  BP (Table I). The younger of these dates indicates that the deposits at and above 4.22 m depth aggraded after  $3540 \pm 110$  BP. Using the calibrated age of this date (3850 cal BP; Table I) and the approximate maximum distance between the contemporary river channel and an isoline extrapolated across the floodplain using the ridge and swale pattern as a guide (Fig. 3), the average rate of past lateral channel migration since 3850 cal BP is estimated to be  $0.08 \text{ m a}^{-1}$ . This represents a maximum rate of migration, since the age of the dated charcoal at 4.22 m depth is likely significantly younger than the initiation of convex bank aggradation at the specific location of section Ju30-1-98, as mentioned above. Despite this, the rate of channel migration is of the same order-of-magnitude as that reported by Brooks (2003b) for a meander near St. Jean Baptiste, which ranged from  $0.04$  to  $0.08 \text{ m a}^{-1}$  over the past 6000 years. Overall, the

rate of migration for the meander at section Ju30-1-98 provides supporting evidence that the Red River meanders have experienced slow rates of lateral channel migration since the mid-Holocene. These rates are significantly lower than those reported for higher energy sand- and gravel-bed rivers in western Canada (see for example, Hickin and Nanson, 1984). The low Red River rates of migration reflect the low unit stream power of the river at bankfull discharge ( $\sim 5 \text{ Wm}^{-2}$ ) and the cohesive character of the glaciolacustrine and alluvial deposits along the concave banks (Brooks, 2003b).

#### VERTICAL SEDIMENTATION RATES

The depth-age positions of the samples from sections Se04-1-97, Ju30-1-98, Ju23-1-98, Ju23-2-98, Ju21-2-98 and Ju19-1-98 are depicted in Figure 4. Interpretative lines (fitted by eye) through the data points from each section reveal the general temporal trend of sedimentation. These show an overall decrease in the vertical sedimentation rates towards the top of the banks in four of the six exposures. At depths below 1 m (and as deep as 3 m in some sections), the rates range from  $1.7$  to  $3.7 \text{ mm a}^{-1}$ . The rates vary from  $0.3$  to  $0.8 \text{ mm a}^{-1}$  in the upper portion of the exposures (Fig. 4; Table II). The vertical decrease in rates is interpreted to reflect a shift in

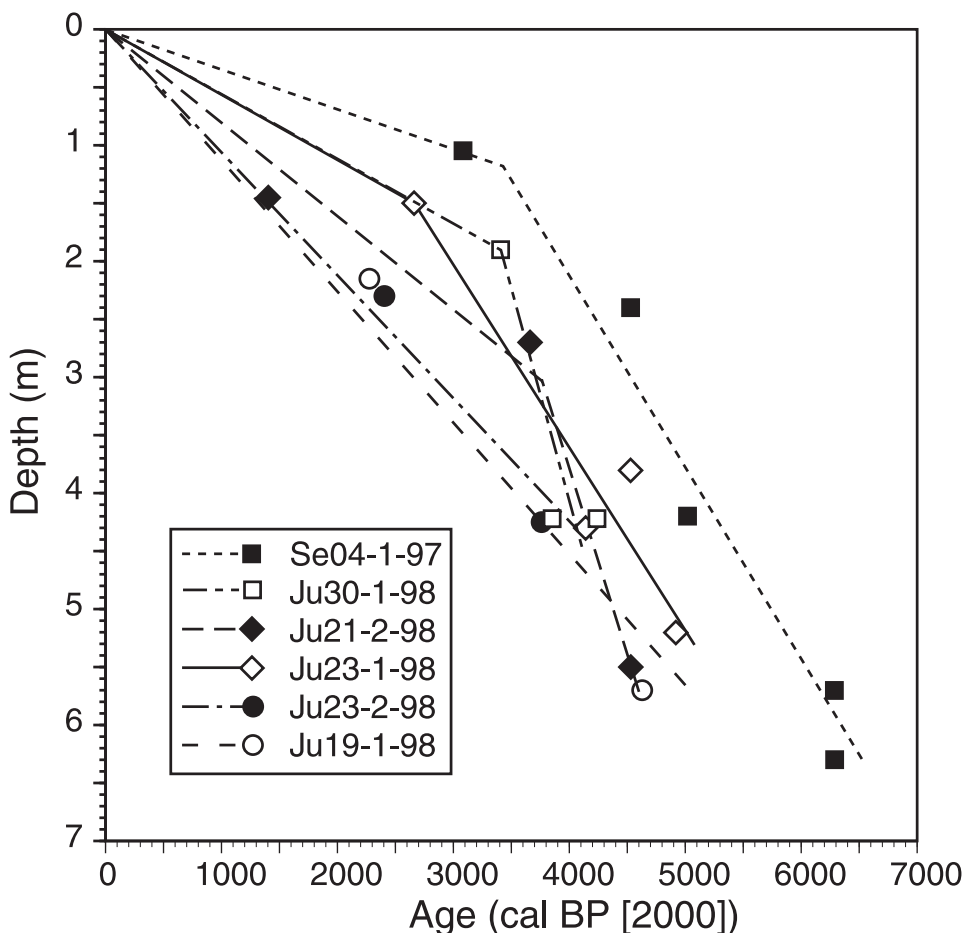


FIGURE 4. Plots of calibrated age versus depth for the dated samples from sections Se04-1-97, Ju30-1-98, Ju23-1-98, Ju23-2-98, Ju21-2-98 and Ju19-1-98. Interpretative lines have been fitted to the data points of each section.

Graphique des âges étalonnés par rapport à la profondeur des échantillons datés et provenant des coupes Se04-1-97, Ju30-1-98, Ju23-1-98, Ju23-2-98, Ju21-2-98 et Ju19-1-98. Les différentes lignes ont été tracées en fonction des données propres à chacune des coupes.

TABLE II

Rates of vertical sedimentation for sections Se04-1-97, Ju30-1-98, Ju23-1-98, Ju23-2-98, Ju21-2-98 and Ju19-1-98

| Section   | Rate for depth range less than ~2 m ( $\text{mm a}^{-1}$ ) | Rate for depth range greater than ~2 m ( $\text{mm a}^{-1}$ ) | Average rate ( $\text{mm a}^{-1}$ ) |
|-----------|--|---|-------------------------------------|
| Se04-1-97 | 0.3  | 1.7   | -                                   |
| Ju30-1-98 | 0.6  | 3.7   | -                                   |
| Ju23-2-98 | -  | -   | 1.1                                 |
| Ju23-1-98 | 0.7  | 1.8   | -                                   |
| Ju21-2-98 | 0.8  | 3.2   | -                                   |
| Ju19-1-98 | -  | -   | 1.1                                 |

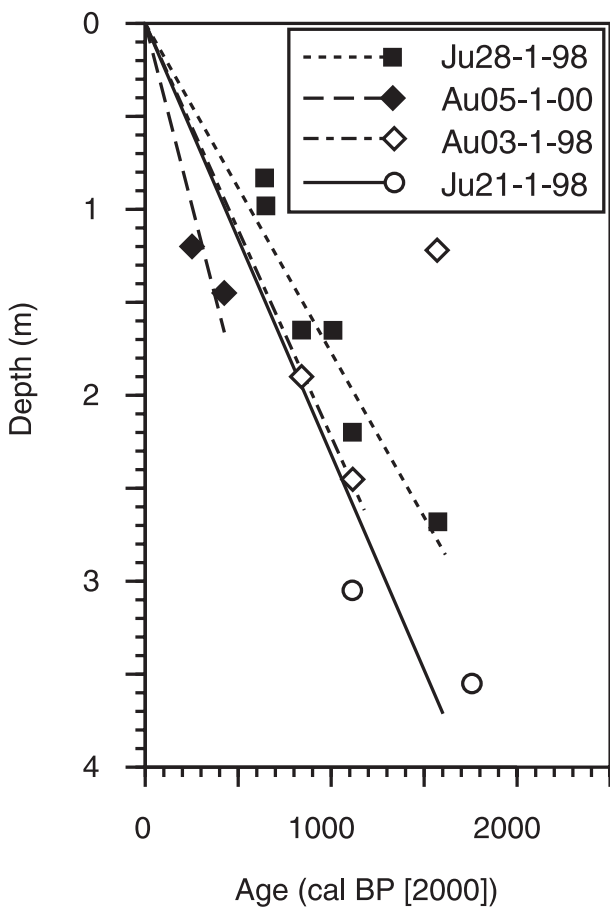


FIGURE 5. Plot of calibrated age versus depth of the dated samples from sections Ju28-1-98, Au05-1-00, Au03-1-98 and Ju21-1-98. Of note, the stratigraphically youngest age from section Au03-1-98 is an outlier, probably based on reworked charcoal, and has not been used to define the line for this dataset.

Graphique des âges établis par rapport à la profondeur des échantillons provenant des coupes Ju28-1-98, Au05-1-00, Au03-1-98 et Ju21-1-98. Noter que la date la plus récente obtenue à la coupe Au03-1-98 est éloignée des autres probablement parce qu'elle a été obtenue à partir de charbon remanié ; elle a été exclue pour la définition de la droite.

depositional environment controlled by the change in lateral and vertical position of the floodplain surface relative to the migrating river channel. Over time the aggrading bank surface would experience a decreasing frequency of inundation because of its increasingly higher relative position above the channel. The higher rates of sedimentation probably represent oblique accretion/overbank sedimentation proximal to the channel with the lower rates representing distal overbank sedimentation on a topographically higher surface (see Brooks, 2003a). The gradational and indistinct transition between the oblique accretion and overbank deposits, as mentioned above, inhibits a definitive correlation between the sedimentation rates and deposit types. The occurrence of paleosols in the upper 1 to 3 m of sections Se04-1-97, Ju30-1-98 and Ju23-1-98 indicates that there has been significant decreases or hiatuses in the vertical accumulation of the distal overbank deposits. Such variations in sedimentation likely are climatically controlled and relate to temporal fluctuations in the frequency-magnitude of Red River floods.

In two sections, Ju23-2-98 and Ju19-1-98, the rates are linear, but are based on only two radiocarbon ages at each section (Fig. 3). The average rates of sedimentation at both sections are about  $1.1 \text{ mm a}^{-1}$ , which falls between the ranges of the upper and lower bank at sections Se04-1-97, Ju30-1-98, Ju23-1-98 and Ju21-2-98 (Table II).

In contrast to the aforementioned sections, the stratigraphically lowest radiocarbon ages in sections Ju28-1-98, Au05-1-00, Au03-1-98 and Ju21-1-98 are late Holocene in age, ranging between 430 and 1760 cal BP, and are positioned in the upper several metres of the bank (Table I). These sections are located at isolated bank slumps along the concave banks of meanders (Au03-1-98 and Ju21-1-98), a convex bank at the entrance to a meander (Ju28-1-98) and a relatively straight section of channel (Au05-1-00). The age-depth positions of the samples are plotted in Figure 5 with interpretative lines through each dataset. The interpretative line for section Au03-1-98 is based on the two deeper ages as the shallowest sample is interpreted to be reworked charcoal, as mentioned above. The interpretative lines reveal linear sedimentation rates that range between  $1.8$  and  $3.9 \text{ mm a}^{-1}$  (Table III), although only that of section Ju28-1-98 is based on more than two data points.

The sedimentation rates from sections Ju28-1-98, Au05-1-00, Au03-1-98 and Ju21-1-98 are significantly greater than those from the upper 1 to 3 m of sections Se04-1-97, Ju30-1-98, Ju23-1-98 and Ju21-2-98 ( $1.8$  to  $3.9 \text{ mm a}^{-1}$  versus  $0.3$  to  $0.8 \text{ mm a}^{-1}$ , respectively; Tables II and III), but are similar to those from the deeper parts of the other sections ( $1.7$  to  $3.7 \text{ mm a}^{-1}$ ; Table II). As an initial hypothesis, the variability in sedimentation rates in the upper portions of the floodplain deposits is inferred to reflect differences in the bank heights relative to the channel and therefore in the frequency of inundation and burial between the two groups of sections. It is difficult to compare the relative heights of the banks due to the distances between the sections (Fig. 1) and different river stage on the day of logging. Qualitatively, however, it was apparent in the field that the bank surfaces at sections Ju28-1-98, Au05-1-00, Au03-1-98 and Ju21-1-98 are situated

TABLE III

*Rates of vertical sedimentation for sections Ju28-1-98, Au03-1-98, Au05-1-00 and Ju21-1-98*

| Section   | Average rate ( $\text{mm a}^{-1}$ ) |
|-----------|-------------------------------------|
| Ju28-1-98 | 1.8                                 |
| Au03-1-98 | 2.3                                 |
| Au05-1-00 | 3.9                                 |
| Ju21-1-98 | 2.3                                 |

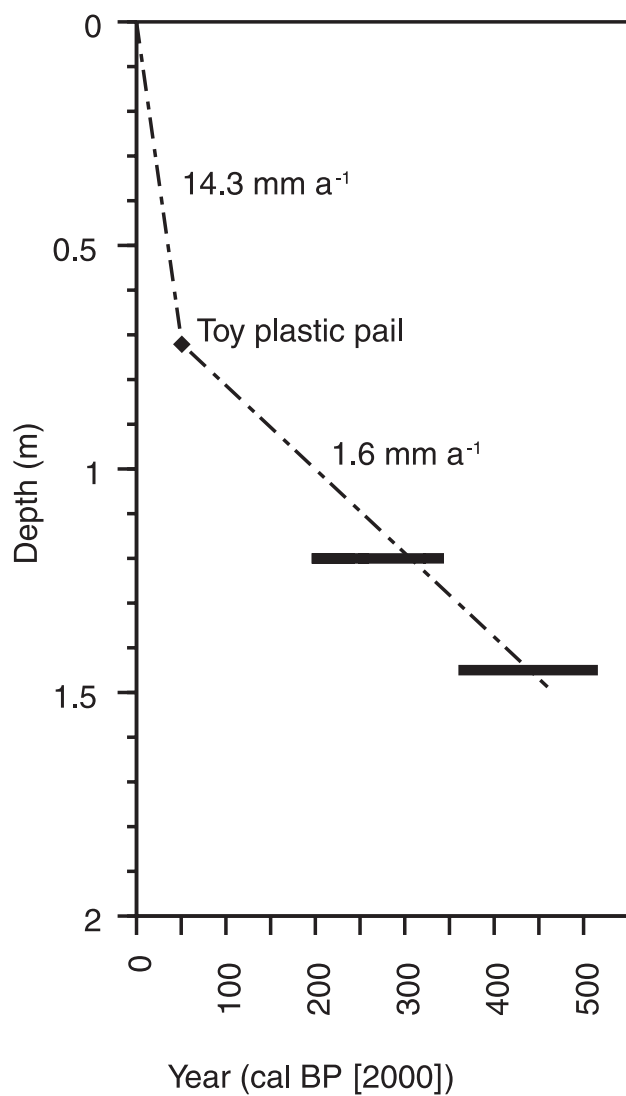


FIGURE 6. Plot of the age versus depth of the calibrated radiocarbon ages ( $1\sigma$  error range) and toy plastic pail from section Au05-1-00. The age of burial of the plastic pail is not known, but a limiting age of AD 1950 has been used.

*Graphique des âges par rapport à la profondeur des points datés au radiocarbone (étalonnage : marge d'erreur de  $1\sigma$ ) et du seau jouet en plastique (coupe Au05-1-00). La date de l'enfouissement du seau n'est pas connue, mais 1950 ap. J.-C. sert de limite.*

lower relative to the channel than those at sections Se04-1-97, Ju30-1-98, Ju23-1-98 and Ju21-2-98, based on high water marks from the freshet. This implies that the bank surfaces at the former group of sections are inundated more frequently and thus are buried more often by overbank deposits than the higher bank surfaces. The similarity of sedimentation rates suggests that these bank surfaces are situated within a depositional environment equivalent to that below 1 to 3 m depth in sections Se04-1-97, Ju30-1-98, Ju23-1-98 and Ju21-2-98.

Rates of vertical sedimentation along the Red River have been estimated in the Winnipeg area by Nielsen *et al.* (1993), based on radiocarbon dated charcoal, bone and shell samples. Most comparable are the rates from their St. Vital and Ravenscourt sites, which represent meandering sections of the river just upstream of the Assiniboine River confluence. Their data yield average sedimentation rates of about 1.3 and 2.0  $\text{mm a}^{-1}$  for the St. Vital and Ravenscourt sites, respectively, over the late Holocene. These rates are consistent with those from sections Ju28-1-98, Au05-1-00, Au03-1-98 and Ju21-1-98 (Table III) and the rates from the deeper portions of sections Se04-1-97, Ju30-1-98, Ju23-1-98 and Ju21-2-98 (Table II).

Additional chronological data from section Au05-1-00 indicates that the modern sedimentation rate may have increased significantly from the longer term average. At this section, a toy plastic pail collected at 0.72 m depth is a 20<sup>th</sup> century artifact and provides a maximum age for the upper 0.72 m of the bank. Using AD 1950 as a limiting age for the pail (approximately the time that plastic was in widespread use in toys; P. Rider, personal communication, November 2002), a plot of the depth versus age of the pail and the  $1\sigma$  error range of the two radiocarbon ages from the section is depicted in Figure 6. This plot reveals that the rates of sedimentation have shifted from 1.6 to 14.3  $\text{mm a}^{-1}$  below and above 0.72 m depth, respectively (Fig. 5). The rate below 0.72 m depth is consistent with the average rates of 1.8 and 2.3  $\text{mm a}^{-1}$  from sections Ju28-1-98, Au03-1-98 and Ju21-1-98, respectively (Table III), but the rate above 0.72 m depth is nearly an order-of-magnitude higher. Although the age of burial for the pail is not known with certainty, if the actual age is in fact younger than AD 1950, then the rate of sedimentation above 0.72 m depth would be greater than 14.3  $\text{mm a}^{-1}$ .

Brooks and Grenier (2001) report higher modern sedimentation rates in a core from the bed of Lake Louise, which occupies a Red River paleochannel near Emerson, based on a single radiocarbon date and a shift in pollen spectra associated with the introduction of European agricultural practices in AD 1880s. The post-1880 rates (2.5  $\text{mm a}^{-1}$ ) were about 10 times higher than those between 1880 and AD 420 (0.24  $\text{mm a}^{-1}$ ). Both of these rates are lower than those from section Au05-1-00, but Lake Louise is located about 2 km west of the Red River, in contrast to section Au05-1-00 which is situated immediately beside the channel. Brooks and Grenier (2001) attribute the increased post-1880 sedimentation to greater fluvial erosion in the landscape due to the introduction and continued usage of European agricultural practices within the drainage basin. In Figure 6, the interval of higher sedimentation rates appears to start considerably after

the 1880s, but this is an artifact of the estimated age of the plastic pail. Additional chronological data is needed from section Au05-1-00 and elsewhere along the river both to confirm the general increase in recent sedimentation rates along the river and to better determine when the increase in sedimentation rate began and whether this relates to the introduction of European agricultural practices.

## CONCLUSIONS

The stratigraphically oldest radiocarbon ages from sections Au07-1-98, Se04-1-97, Ju30-1-98, Ju23-1-98, Ju-23-2-98, Ju21-2-98 and Ju19-1-98 are mid-Holocene in age. In combination with a single ridge and swale sequence on the floodplain, these ages are consistent with the notion that most of the Red River meanders have only experienced a single episode of lateral channel migration. The rate of lateral channel migration of the meander where section Ju30-1-98 is situated has averaged up to  $0.08 \text{ m a}^{-1}$  since 3850 cal BP. This rate, as well as those reported from elsewhere along the Red River in southern Manitoba, is significantly lower than those associated with higher energy sand- and gravel-bed rivers.

In sections Se04-1-97, Ju30-1-98, Ju23-1-98 and Ju21-2-98 there is a marked decrease in the rate of vertical sedimentation from  $1.7 \text{ mm a}^{-1}$  to  $0.3 \text{ to } 0.8 \text{ mm a}^{-1}$  at 1 to 3 m depth. This decrease in sedimentation is interpreted to represent a shift from oblique/proximal overbank accretion to distal overbank deposition. It probably relates to the relative height of the aggrading surface above the river channel and an associated decrease in frequency of inundation.

The average rates of vertical sedimentation in sections Ju28-1-98, Au05-1-00, Au03-1-98 and Ju21-1-98 are similar to the rates below 1 to 3 m in sections Se04-1-97, Ju30-1-98, Ju23-1-98 and Ju21-2-98. The bank surface of the former group of sections is considered to represent an equivalent depositional environment to the deeper portions of the sections Se04-1-97, Ju30-1-98, Ju23-1-98 and Ju21-2-98.

Modern sedimentation rates in section Au05-1-00 increase markedly from  $1.6 \text{ mm a}^{-1}$  to  $14.3 \text{ mm a}^{-1}$ , based on the estimated age of a buried toy plastic pail and two radiocarbon ages. This increase may be part of a trend of enhanced fluvial erosion caused by the large-scale introduction and continued usage of European agricultural practices in the Red River Valley during the 19<sup>th</sup> and 20<sup>th</sup> centuries, but additional chronological data are needed to substantiate this.

## ACKNOWLEDGEMENTS

This work was funded in part by the International Red River Basin Task Force. Logistical support of the Manitoba Geological Survey is gratefully acknowledged. I thank P. Rider, Canadian Museum of Civilization, for discussions on the use of plastic in toys. Comments from J. Desloges, A. Plouffe and

H. Saunderson on early drafts are appreciated. The aerial photograph in Figure 3 (© 1980, Her Majesty the Queen in Right of Canada) reproduced from the collection of the National Air Photo Library with permission of National Resources Canada.

## REFERENCES

- Brooks, G.R., 2003a. Alluvial deposits of a mud-dominated stream; the Red River, Manitoba, Canada. *Sedimentology*, 50: 441-458.
- \_\_\_\_\_, 2003b. Holocene lateral channel migration and incision of the Red River, Manitoba, Canada. *Geomorphology*, 54: 197-215.
- Brooks, G.R. and Grenier, A., 2001. Late Holocene Pollen Stratigraphy of Lake Louise, Manitoba. *Geological Survey of Canada, Ottawa, Current Research 2001-B1*, 7 p.
- Brooks, G.R. and Nielsen, E., 2000. Red River, Red River Valley, Manitoba. *The Canadian Geographer*, 44: 304-309.
- Hickin, E.J. and Nanson, G.C., 1984. Lateral migration rates of river bends. *Journal of Hydraulic Engineering*, 110: 1557-1567.
- Johnston, W.A., 1946. Glacial Lake Agassiz, with Special Reference to the Mode of Deformation of the Beaches. *Geological Survey of Canada, Ottawa, Bulletin 7*, 20 p.
- Lian, O.B. and Brooks, G.R., 2004. Optical dating studies of alluvium and hearth-like features from Red River Valley, southern Manitoba, Canada. *The Holocene*, 14.
- Nanson, G.C. and Croke, J.C., 1992. A genetic classification of floodplains. *Geomorphology*, 4: 459-486.
- Nielsen, E., McKillop, W.B. and Conley, G.G., 1993. Fluvial sedimentology and paleoecology of Holocene alluvial deposits, Red River, Manitoba. *Géographie physique et Quaternaire*, 47: 193-210.
- Page, K.J., Nanson, G.C. and Frazier, P.S., 2003. Floodplain formation and sediment stratigraphy resulting from oblique accretion on the Murrumbidgee River, Australia. *Journal of Sedimentary Research*, 73: 5-14.
- Rannie, W.F., 1990. The Portage la Prairie "floodplain fan", p 179-192. *In A.H. Rachoeki and M. Church, eds., Alluvial Fans. A Field Approach*. John Wiley, Chichester, 391 p.
- Rannie, W.F., Thorleifson, L.H. and Teller, J.T., 1989. Holocene evolution of the Assiniboine River paleochannels and Portage la Prairie alluvial fan. *Canadian Journal of Earth Sciences*, 26: 1834-1841.
- Stuiver, M. and Reimer, P.J., 1993. Extended  $^{14}\text{C}$  data base and revised calib 3.0  $^{14}\text{C}$  age calibration program. *Radiocarbon*, 35: 215-230.
- Stuiver, M., Reimer, P.J., Bard, E., Beck, J.W., Burr, G.S., Hughen, K.A., Kromer, B., McCormac, G., van der Plicht, J. and Spurk, M., 1998. INTCAL98 radiocarbon age calibration, 24,000-0 cal B.P. *Radiocarbon*, 40: 1041-1083.
- Teller, J.T., 1976. Lake Agassiz deposits in the main offshore basin of southern Manitoba. *Canadian Journal of Earth Sciences*, 13: 27-43.
- \_\_\_\_\_, 2001. Formation of large beaches in an area of rapid differential isostatic rebound: The three-outlet control of Lake Agassiz. *Quaternary Science Review*, 20: 1649-1659.
- Teller, J.T. and Clayton, L., ed.. 1983. Glacial Lake Agassiz. *Geological Association of Canada, Waterloo, Special Paper 26*, 451 p.
- Teller, J.T., Thorleifson, L.H., Matile, G. and Brisbin, W.C., 1996. Sedimentology, geomorphology and history of the central Lake Agassiz basin (Field Trip B2). *Geological Association of Canada/Mineralogical Association of Canada, 1996 Joint Annual Meeting (Winnipeg, Manitoba)*, Field trip guidebook, Winnipeg, 101 p.
- Upham, W., 1895. The Glacial Lake Agassiz. *United States Geological Survey, Washington, Monograph 25*, 658 p.